

We are IntechOpen, the world's leading publisher of Open Access books Built by scientists, for scientists

4,800

Open access books available

122,000

International authors and editors

135M

Downloads

Our authors are among the

154

Countries delivered to

TOP 1%

most cited scientists

12.2%

Contributors from top 500 universities



WEB OF SCIENCE™

Selection of our books indexed in the Book Citation Index
in Web of Science™ Core Collection (BKCI)

Interested in publishing with us?
Contact book.department@intechopen.com

Numbers displayed above are based on latest data collected.

For more information visit www.intechopen.com



Cubic SiC Nanowires: Growth, Characterization and Applications

Giovanni Attolini, Francesca Rossi, Filippo Fabbri, Matteo Bosi,
Giancarlo Salviati and Bernard Enrico Watts
*IMEM-CNR Institute
Italy*

1. Introduction

Since the introduction of carbon nanotubes in 1992, the study of one-dimensional nanomaterials, which includes metallic, magnetic, semiconducting and oxide compounds, has attracted considerable interest, especially as regards nanowires (NW), nanobelts and nanorods [Kolasinski, 2006].

The main interests of this research are in the realization of nanoelectronic devices (e.g. nano field-effect transistors), nano-electromechanical systems, and nano-sensors exploiting high selectivity and compatibility with biological systems. Nanostructures may present very different characteristic and novel properties with respect to the corresponding bulk material, and they have important physical and chemical properties, in particular large specific surface/volume ratio and quantum size effects, which permit many applications such as nanoscale devices, sensors and scanning probes not possible with standard structures.

Silicon carbide (SiC) has gained importance as both a coating and a structural material for Micro Electro Mechanical Systems (MEMS) (Sarro, 2000; Mehregany et al, 2000). SiC is a wide bandgap semiconductor used for high temperature, high power applications and radiation-hard environments. The high Si-C bond energy confers a high Young's modulus and hence mechanical toughness and high fracture strength (Li and Bhushan, 1999); moreover, it is chemically inert to the most corrosive and erosive chemicals and is biocompatible (Willander et al. 2006; Casady and Johnson 1996; Yakimova et al. 2007). More than 100 polytypes of SiC exist but the SiC cubic phase (3C-SiC) has drawn particular attention because it can be deposited on Si (Marshall et al. 1973).

The combination of these distinctive physical, chemical and mechanical properties of SiC and the possibility to synthesize SiC NW make this material an excellent candidate for the design and fabrication of nanodevices.

Surface functionalization introduces specific chemical functional groups onto a surface, in order to tailor its properties to specific needs. Functionalization of NW is nowadays a burgeoning field of activity, and motivates researchers involved in nanotechnology and related activities: defining a specific molecule/NW interface, suitable for selective bonding to a chosen chemical species, is a key step of the development of nano-objects tuned by the physical and chemical properties of molecules, and may have notable application in sensing and biosensing.

Source: Nanowires, Book edited by: Paola Prete,
ISBN 978-953-7619-79-4, pp. 414, March 2010, INTECH, Croatia, downloaded from SCIYO.COM

Functionalized 3C-silicon carbide NW have the potential to act as highly sensitive detector elements in bio-chemical field (Yakimova et al., 2007).

Many methods are currently being used to prepare SiC-NW (pure or with a SiO₂ shell) on silicon substrates using a catalyst, including chemical vapour deposition, vacuum evaporation of SiC, direct synthesis from Si and C powders.

In this paper we will present a brief review of growth methods used to obtain cubic silicon carbide NW, both with and without SiO₂ shell, and our results on the NW growth and characterization of morphological, structural and optical properties by SEM, TEM, CL and Raman.

Finally we will review some of the possible applications for nanodevices.

2. A brief review of NW growth methods

Different growth methods have been developed to prepare NW of different materials, and several theoretical models have been proposed to explain the growth mechanisms.

Semiconductor NW are generally synthesized via a Vapor-Liquid-Solid (VLS) process (Wagner and Ellis, 1964), a process that can be divided in three main steps: a) formation of a small liquid droplet on the surface of the substrate, b) supersaturation of the liquid by the incorporation of gaseous precursors and c) subsequent nucleation and growth of the NW from the liquid-solid interface.

Small metal clusters are deposited by different techniques on the substrate surface, forming nanosized dots.

In a second step, a gas of the proper precursors flows through the reaction tube and, when in contact with the metal droplets, the precursor deposits on the liquid surface and forms an alloy. A continuous incorporation of the precursor leads to a supersaturation of the desired compounds and as a consequence to the NW growth at the solid-liquid interface.

With other growth techniques it is possible to realize NW without a metal catalyst on the substrate surface, by thermal evaporation of a suitable source near its melting point and subsequent deposition at cooler temperature. This mechanism is called "vapor-solid" (VS) growth and has been mainly used to synthesize metal oxide and some semiconductor nanomaterials (Wang et al., 2008). It is often called self-catalytic growth, since in this case one component of the gaseous atoms might play the role of the catalyst.

3C-SiC/SiO₂ core-shell NW have been synthesized both by a direct heating method using WO₃ and graphite mixed powder as starting material and Ni as catalyst (Bark et al., 2006) and from a mixture of activated carbon and sol-gel derived silica embedded with Fe nanoparticles (Liang et al., 2000).

They are also obtained using iron catalyst by chemical vapor reaction in a mixture of milled Si and SiO₂ powders and C₃H₆ as raw materials in a graphite reaction cell (Meng et al., 2007).

Alternatively, a CVD method can be employed making use of Fe as catalyst and methane as precursor (Zang et al., 2002).

A high yield core/shell SiC/SiO₂ NW production method without the use of catalyst was developed starting from raw powders of Si via an oxide assisted thermal evaporation process (Khongwong et al., 2009).

Core-shell SiC NW have also been synthesized from carbon monoxide using Ni catalyst by carbothermal reduction method (Attolini et al., 2008).

Pure 3C-SiC NW, without shell and free from impurities with the exception of those related to the catalyst at the tip, have been prepared as follows:

3C-SiC NW were deposited on silicon substrate by metalorganic chemical vapor deposition (MOCVD) by using Ni, Au, Fe as catalysts and dichloromethylvinylsilane or methyltrichlorosilane as precursors (Kang et al., 2004; Takai et al., 2007; Yang et al., 2004; Choi et al., 2004; Seong et al., 2004).

The CVD approach consists in flowing the reactants with a carrier gas in a reaction tube inserted in a furnace where either (100) or (111) oriented silicon substrate are placed.

Polycarbosilane (PCS) was used as a precursor to grow porous silicon carbide ceramics with embedded β -SiC NW (Zhu et al., 2005).

Single β -SiC NW were grown through annealing of polycrystalline SiC layer in hydrogen atmosphere at 1150°C (Yang et al., 2006).

Table 1 gives a brief overview of the different methods with the main parameters used in SiC NW growth.

Methods	Chemical Vapor Deposition (including Metal Organic Vapor Phase Epitaxy, Chemical Vapor Reaction, Chemical Vapor Infiltration), Physical Vapor Deposition, Sputtering
Precursors	Methyltrichlorosilane, Dichloromethylsilane, Methane, Propane, Silane, Diethylsilane
Starting materials	Si+SiO ₂ with methane; Si+C; SiC powder;
Substrates	(100), (111) Silicon
Catalyst	Ni, Fe, Au, Pt, Pd, Fe/Co, Al
Growth temperatures range	From 1000 to 1400 °C

Table 1. Typical methods and conditions to prepare 3C-SiC NW

3. Experimental

In our laboratory we obtained 3C-SiC NW with three different growth methods:

1. core-shell NW were obtained using carbon oxide in an open tube;
2. SiC NW were synthesized in a heated quartz tube using carbon tetrachloride;
3. SiC NW were grown in a VPE reactor with silane and propane as precursors.

In this section, we will describe these growth procedures and the characterization of the NW in detail.

The morphological and optical characterizations of the as-grown NW were performed by acquiring secondary electron images in an S360 Cambridge Stereoscan Scanning Electron Microscope (SEM) equipped with a Gatan MonoCL2 system with photomultiplier detector to collect Cathodoluminescence (CL) spectra. The structural and compositional analyses were performed by Transmission Electron Microscopy (TEM) in a JEOL 2200FS working at 200 kV, equipped with an in-column Ω filter, a High Angle Annular Dark Field (HAADF) detector for Z-contrast imaging and an Energy-Dispersive X-Ray (EDX) detector for elemental mapping and EDX spectroscopy.

Micro-Raman scattering measurements were performed at room temperature (RT) with a 100x objective and a 532 nm excitation light. The spectrum resolution was about 0.2–0.3 cm⁻¹.

3.1 Growth and characterization of core-shell NW

The growth of 3C-SiC core-shell NW on Si substrates was performed in an open-tube configuration by flowing carbon oxide and nitrogen or argon as carrier gases.

The growth procedure is the following:

- (100) oriented silicon substrates are cleaned in organic solvents with an ultrasonic bath, dipped in a nickel-salt solution and dried in an oven at 60 °C before being placed into the reactor;
- the substrate is placed in an open tube inside a horizontal furnace, previously purged with inert gas to remove air. The central position of the furnace is selected as a zone of constant temperature;
- the temperature is raised to 1100°C and, after temperature stabilization, carbon oxide is introduced into the tube. The growth time was varied from 1 to 60 minutes, while the gas flow was kept constant in all the experiments.

The NW grow on the Ni-covered substrate areas and are arranged in dense forests (see representative SEM images in Fig. 1), with a quite narrow diameter distribution and with lengths up to several tens of microns. A round-shaped tip is observed on the NW, as discussed in the following.

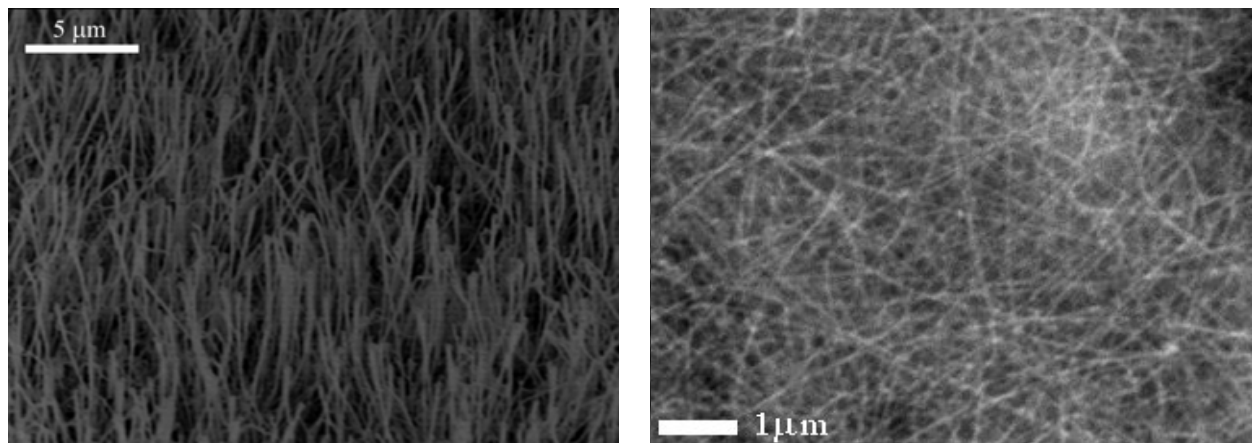


Fig. 1. SEM images of 3C-SiC/SiO₂ core-shell NW. a) 45°- tilted view, showing a good vertical alignment of the NW, b) planar view, showing the quite uniform NW diameter.

Compositional analyses performed by energy filtered TEM and HAADF imaging (see Fig. 2) highlighted the core/shell structure of the NWs. Fig. 2a reports a zero-loss filtered image of a typical wire, showing the crystalline core and the amorphous shell. Elemental mapping (see Fig. 2b-e) confirms the complementary distribution of carbon and oxygen, in the SiC core and in the oxide shell respectively. The oxygen to silicon ratio in the shell, as estimated by EDX point spectra, is very close to two, allowing to identify the shell as silicon dioxide. Further, EDX maps and HAADF images acquired in the tip region (see Fig. 3) confirm the presence of a high-Z nickel-containing particle on top of the NWs, consistently with a VLS growth process.

Structural studies were performed by HRTEM on the NW core. The symmetry of the crystal (inset in Fig.4a) and the lattice spacings identify the structure as 3C-SiC, with <111> growth axis. As reported in Fig. 4a, quite long segments grow almost free of planar defects.

However, the insertion of (111) stacking faults and the occurrence of local stacking sequences of 2H, 4H and 6H polytypes is observed in some areas (Fig. 4b). These results are consistent with the wide literature on planar defects and phase transitions in 3C-SiC whiskers (Seo et al., 2000; Yoshida et al., 2007).

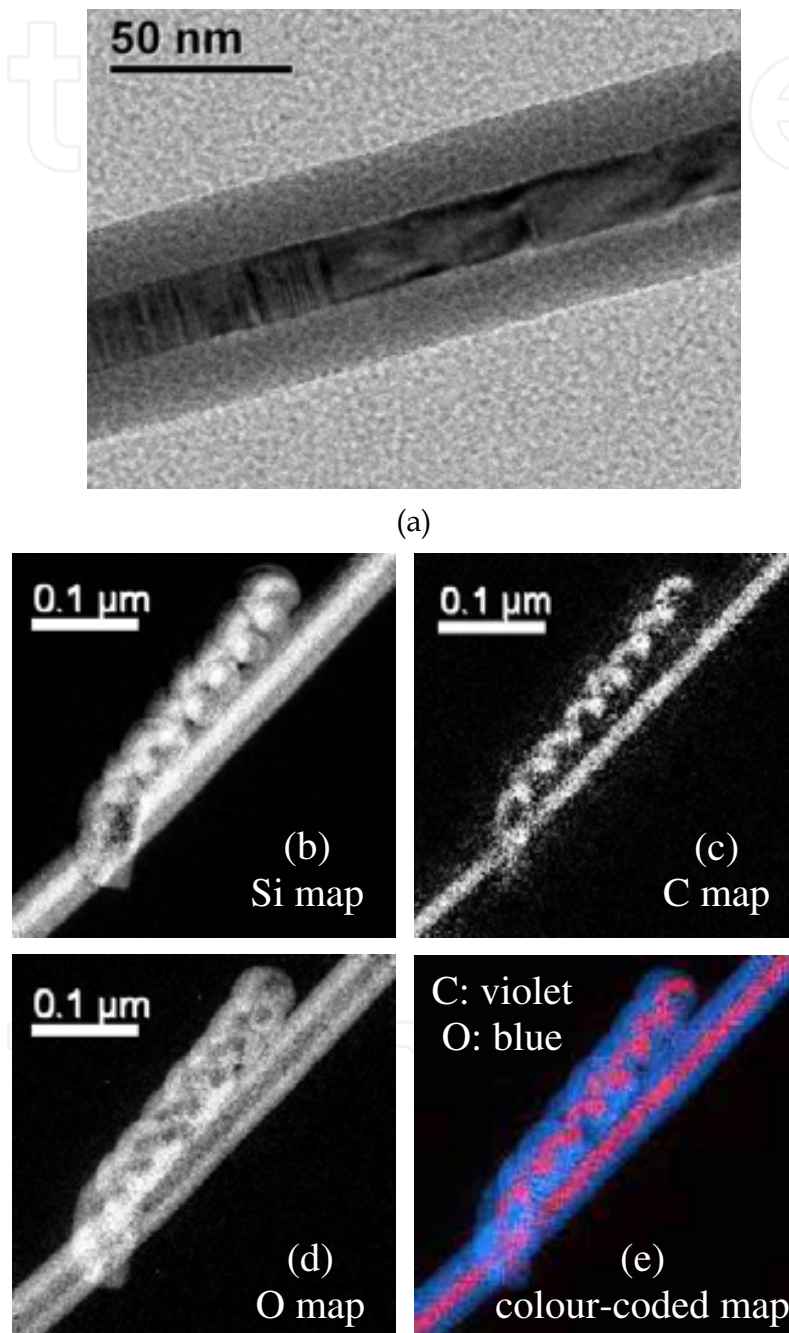


Fig. 2. (a) zero-loss filtered TEM image, evidencing the SiC/SiO₂ core/shell structure, (b)-(d) elemental maps computed from energy-filtered images with the 3 window method. The L_{2,3} silicon edge and the K carbon and oxygen edges have been used for the energy filtering. The map in (e) is obtained by color-mix of the C and O maps.

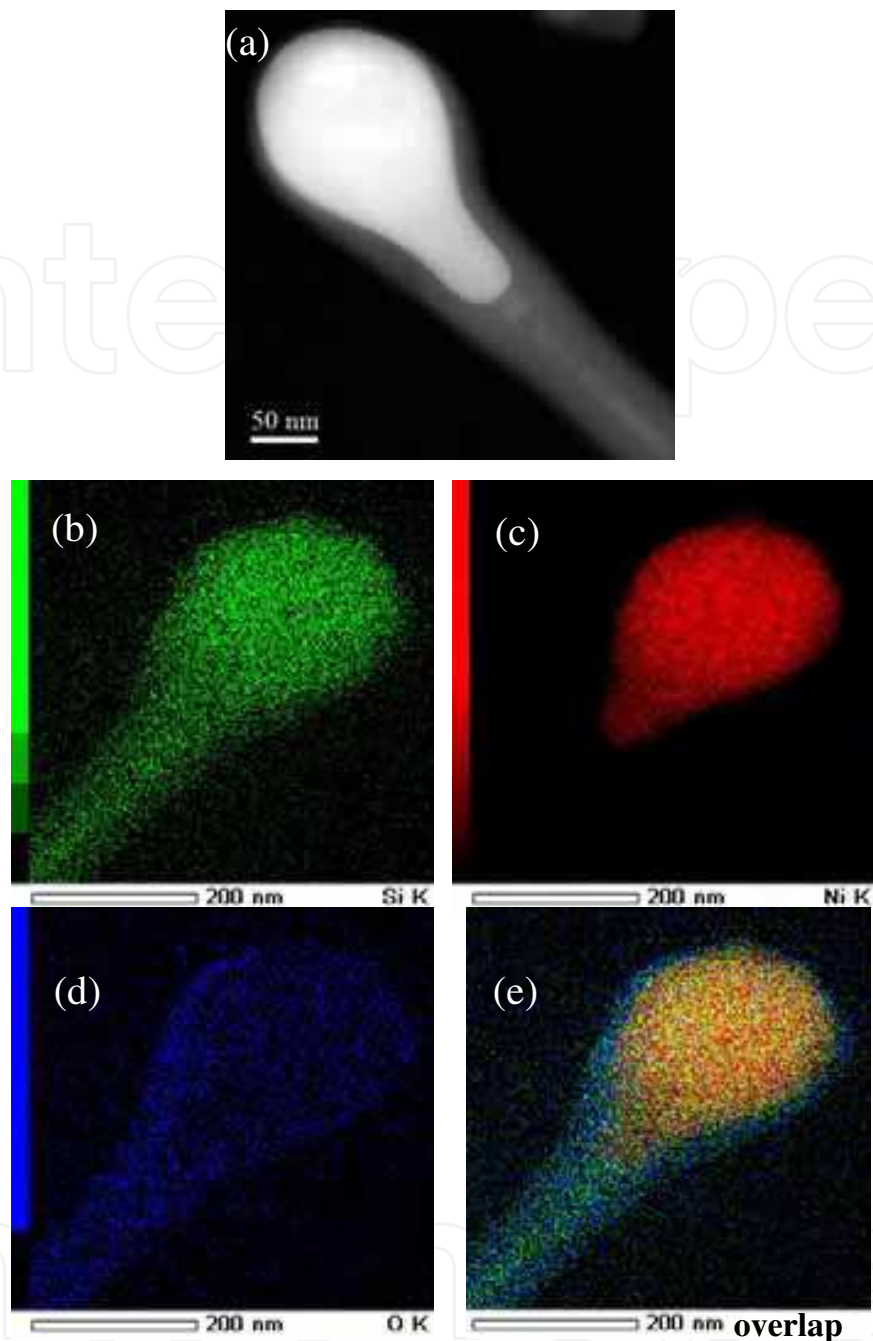


Fig. 3. HAADF image (a) and EDX maps (b-d) showing the distribution of silicon, nickel and oxygen in the tip region of a typical nanowire. (e) is obtained by colour-mix of the maps in (b)-(d).

X-Ray Diffraction (XRD) measurements (see Fig. 5) confirmed the presence of several 3C-SiC peaks, while no evidence of other polytypes phases was observed. A weak shoulder detected on (111) peak at 33.7° could be related to the presence of stacking faults. After a Reitveld refinement carried out using the MAUD program, a value of 4.361 \AA has been calculated for the lattice parameter, in good agreement with the expected value for the β polytype.

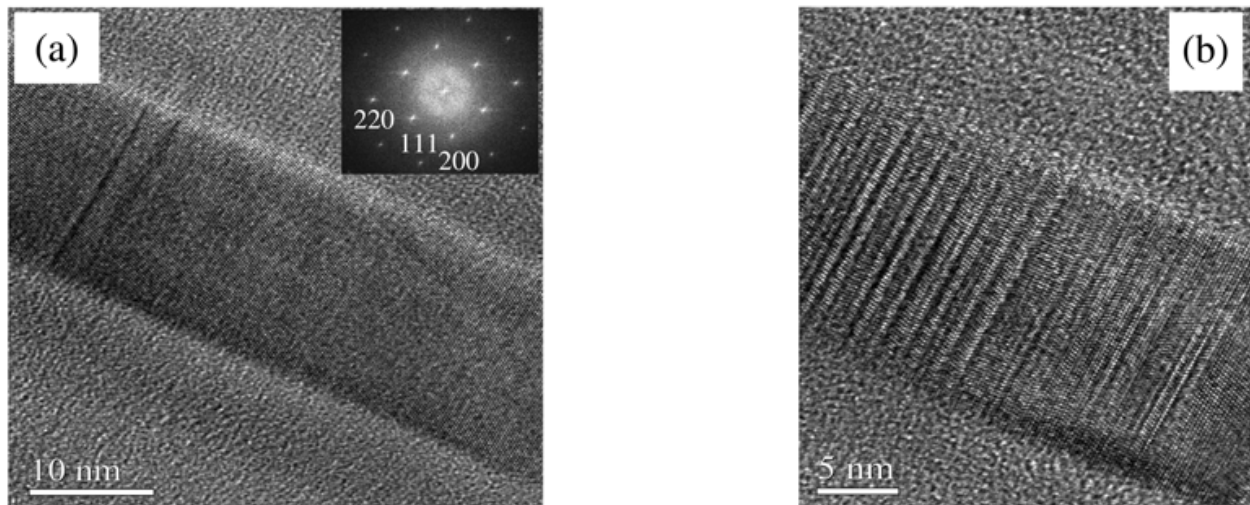


Fig. 4. HRTEM images in [110] zone axis of the 3C-SiC crystalline core: (a) segment almost free of planar defects, (b) defective area. Inset in (a) shows the fast Fourier transform.

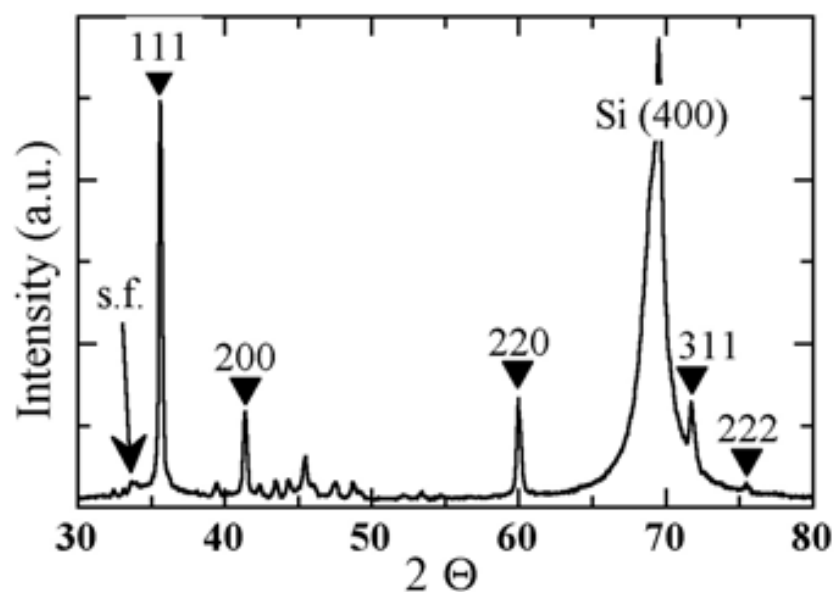


Fig. 5. XRD pattern of a NW sample on a 100 Si substrate. The 3C-SiC peaks (∇) and the extra stacking fault peak (s.f.) are indexed.

The lattice parameter was also analysed by micro-Raman experiments. As shown in Fig. 6, vibrational modes due to the shell and the TO and LO phonon modes of the β -SiC core were revealed. The latter are detected at 797.3 and 976.2 cm^{-1} respectively, slightly shifted from the expected 3C-SiC bulk values. The positions of Raman modes are known to shift because of lattice mismatch (Zhu et al., 2000) and it is possible to estimate the value of $\Delta a/a_0$ from the following equations (Nakashima & Harima, 1997):

$$\omega(\text{TO}) = 796.5 + 3734 \cdot \left(\frac{-\Delta a}{a_0} \right) \quad (1)$$

$$\omega(LO) = 973.0 + 4532 \cdot \left(\frac{-\Delta a}{a_0} \right) \quad (2)$$

We estimated $\Delta a/a_0$ of the order of -0.02% and -0.07% from the TO and LO mode respectively, corresponding to $-\Delta a$ of the order of 10^{-3} Å. The longitudinal variation is slightly higher than the transverse, consistently with the NW geometry. Some broadening of the SiC phonon modes was observed (e.g. TO-FWHM= 4 cm^{-1}) and ascribed to lattice imperfections.

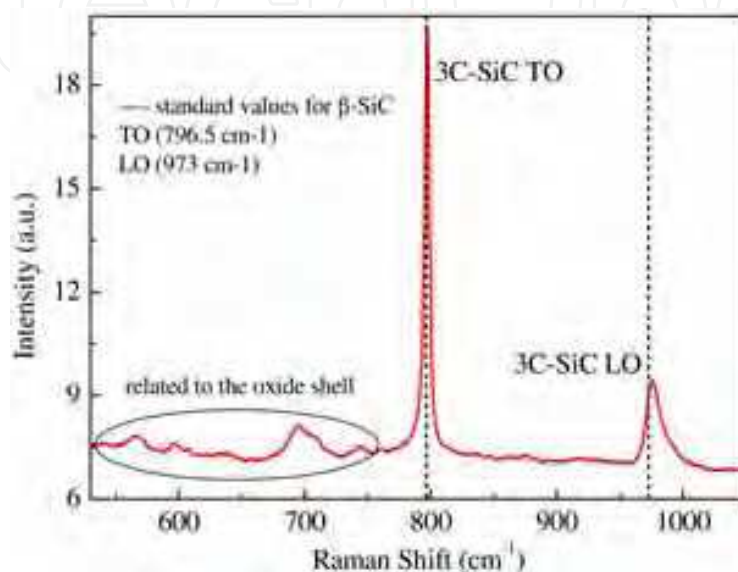


Fig. 6. Raman spectrum of core/shell NW.

Cathodoluminescence experiments were performed to investigate the optical properties of the core/shell NW. A broad room temperature emission, with an intense above-band-gap component, was detected (Fig. 7). By Gaussian deconvolution, the 3C-SiC near-band-edge (NBE) indirect transition was identified at 2.25 ± 0.5 eV, while a second intense band was revealed at about 2.7 eV (blue band).

Above-band-gap luminescence from cubic SiC whiskers and nanocrystallites has been reported in the literature (Xi et al., 2006), but the contribution of a SiO_2 related emission in this spectral region (McKnight & Palik, 1980) has to be considered. In our samples, size-dependent CL studies on single NWs do not give clear evidence of quantum-confinement effects.

Electron beam irradiation effects (Fig. 7a-c) were studied to investigate the blue luminescence. The electron beam in the SEM was kept continuously impinging on the sample and CL spectra were acquired every minute until a total irradiation time of 1 hour. The results of this experiment are reported in Fig. 7c, showing the CL intensity evolution for the two main Gaussian components. The SiC-related emission stays almost constant, while the blue luminescence increases till saturation as a function of the irradiation time. This is consistent with an attribution of the 2.7 eV band to oxygen-deficiency-centres ODC(II) in the silicon dioxide (Skuja, 1998).

Further experiments on the core/shell NW geometry were aimed to study the selective removal of the silicon dioxide layer by etching. A long growth time (1 hour) was selected, to allow the synthesis of a larger amount of NW and the formation of a thicker shell. The

sample was then submitted to etching treatments in HF:H₂O (1:3) solution, and room-temperature CL spectra were acquired at different etching steps (Fig. 8).

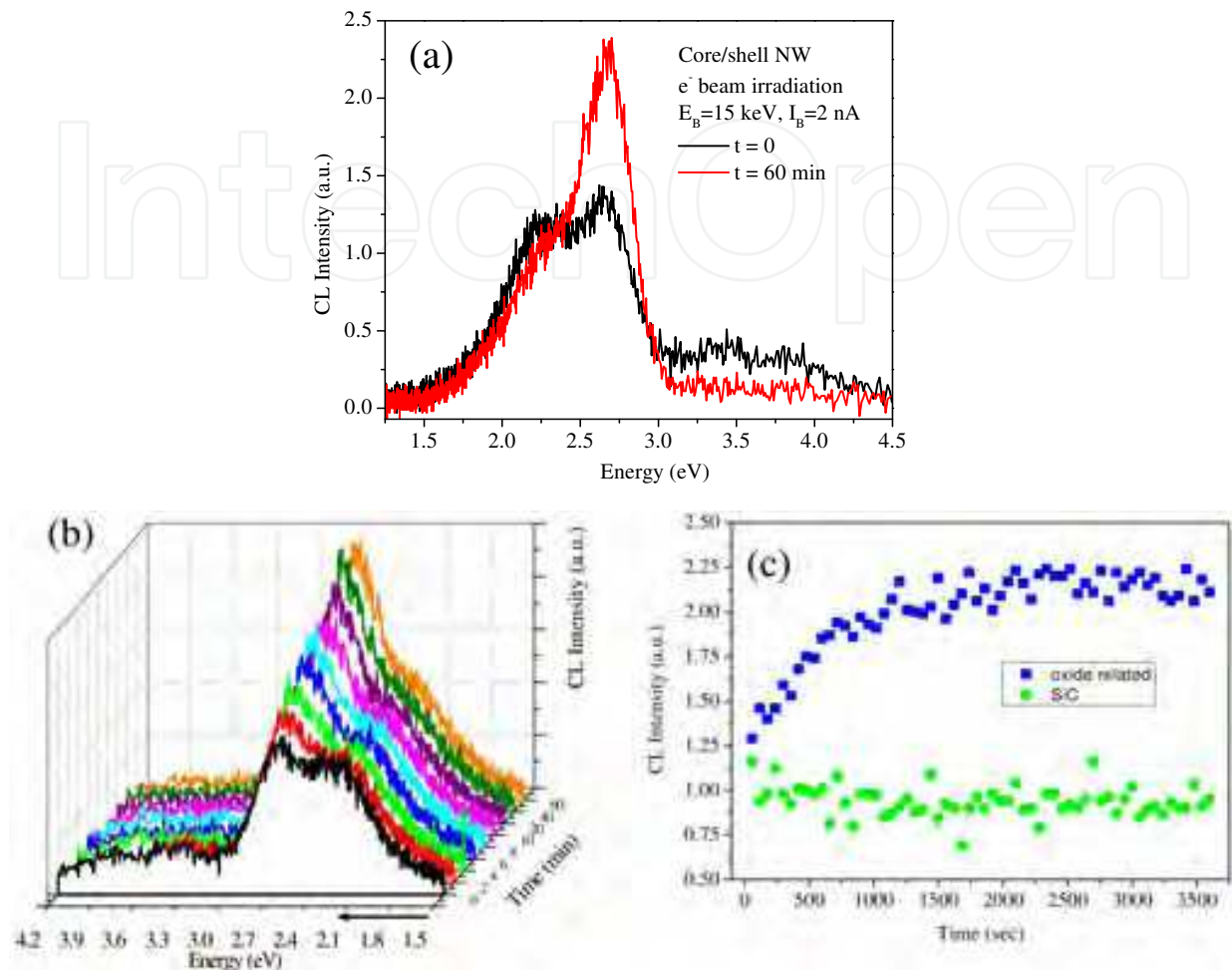


Fig. 7. Room temperature CL spectra of core/shell NW. The spectral evolution after 1 h exposure to the electron beam in the SEM at accelerating voltage of 15 KeV and beam current of 2 nA is reported in (a). Systematic spectra have been acquired as a function of the irradiation time (b), and the time-evolution of the CL intensity is reported in (c) for the two Gaussian components due to the SiC core (circles) and the shell layer (squares).

In these conditions the as-grown NW showed the SiC-NBE and the SiO₂-ODC related emissions discussed above, convoluted with additional bands peaked at about 1.98 eV, 2.55 eV, and 3.15 eV. In agreement with literature data, the 1.98 eV shoulder on the low energy side was assigned to the presence of substitutional oxygen on carbon site (O_C defects), unintentionally incorporated in the silicon carbide lattice [Gali et al, 2002; Kassiba et al., 2002]. The high-energy emission at 3.15 eV could be related to the nanometric inclusions of hexagonal SiC polytypes with $E_{G-6H} = 3.15$ eV, $E_{G-4H} = 3.24$ eV (Bechstedt et al., 1997) as observed by high-resolution TEM (Fig. 4). As for the 2.55 eV band, it was tentatively ascribed to interface states related to carbon clusterization at the core/shell interface (Afanas'ev et al., 1996), suggested also by XPS data (not shown here).

A decrease of the whole CL emission was observed as an effect of the etching treatments (Fig. 8a). In particular, the SiO₂ related bands showed an exponential decay as a function of

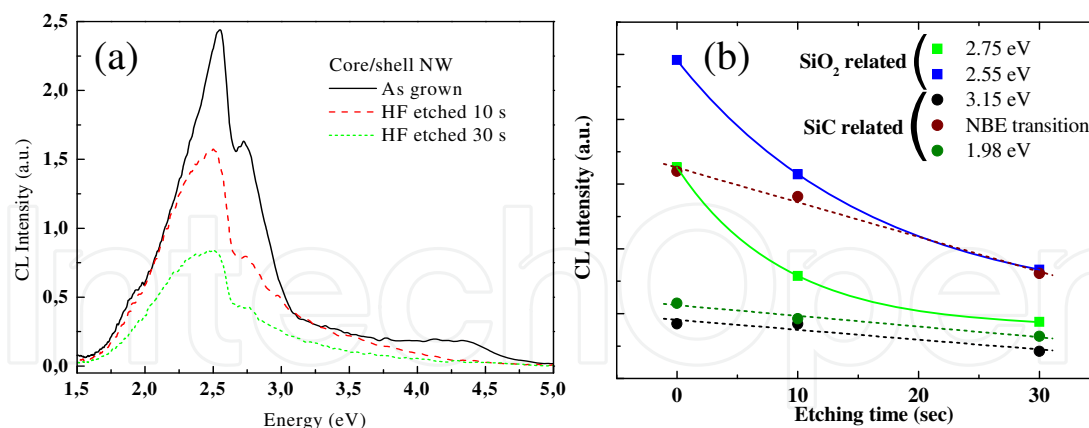


Fig. 8. CL spectra of single NW at different HF etching steps (a) and intensity evolution as a function of the etching time (b). The silicon dioxide and the silicon carbide related emissions show different decays.

the etching time, while the SiC related emissions showed a linear decrease (Fig. 8b). The SiO₂ related emissions decrease in intensity due to material removal. On the contrary, the chemical inertness of the silicon carbide to the hydrofluoric acid etching ensures that the decrease of the SiC related emissions has a different origin. A peculiar relationship between the removal of the silicon dioxide and the decrease of the core luminescence can be hypothesized, as discussed in the following.

It is possible to propose a model to explain why the presence of the silicon dioxide shell increases the radiative recombination in the silicon carbide core. A type I band alignment (Pistol & Pryor, 2008) of 3C-SiC and SiO₂ can be hypothesized, with conduction and valence band-offsets $\Delta E_c = 3.6$ eV and $\Delta E_v = 2.9$ eV (Afanas'ev et al, 1996). In this framework, the carriers generated by the electron beam in the shell diffuse into the core, and here recombine according to the allowed transitions in 3C-SiC. The diffusion of the carriers could be considered as an energy transfer from the shell to the core, an effect that has been observed for semiconductor nanoparticles (Louis et al., 2006) but not yet in NW. In our system, the amorphous shell results to be beneficial to enhance the luminescence intensity of the crystalline core, preferentially the SiC NBE radiative recombination. Besides the effectiveness as a carrier injector region, this could be partly related to the fact that the shell can act as a passivation layer to reduce the non-radiative recombination related to surface states, likewise in the case of entirely crystalline core/shell systems such as GaAs-based NWs (Skold et al. 2005; Jabeen et al. 2008; Tomioka et al., 2009).

3.2 Growth of NW using carbon tetrachloride

A fused silica reaction tube is placed inside an external liner and uniformly heated in a resistance furnace as shown in Fig. 9. The reaction tube is connected to a gas inlet through which a gaseous mixture of N₂-CCl₄ flows, obtained by flowing N₂ into a bubbler containing CCl₄ at 293 K. (100) oriented silicon substrates are cleaned in organic solvents with an ultrasonic bath, dipped in a nickel-salt solution, dried in an oven at 60 °C and put inside the reaction tube.

The air is completely purged by flowing nitrogen. The furnace is heated to 1000 °C while flowing the N₂-CCl₄ mixture and held at this temperature for a growth time of 30 minutes.

The furnace is then switched off, the tube is removed and cooled down to room temperature.

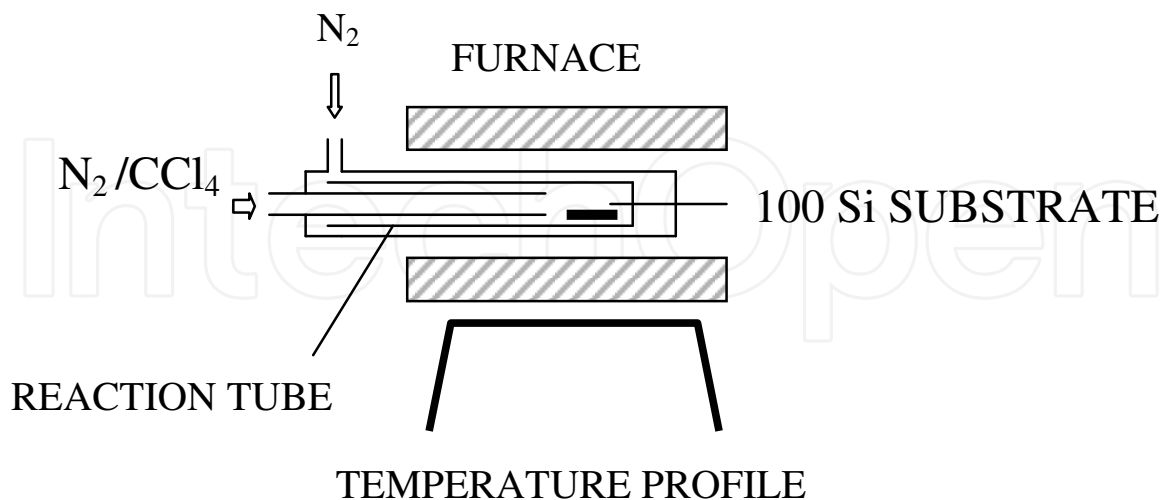


Fig. 9. Schematics of the experimental apparatus for the growth of NW with carbon tetrachloride.

In this case the NW synthesis is obtained by a three step process, consisting in:

1. thermal decomposition of CCl_4
2. reaction of chlorine decomposition products with silicon, both on substrate surface and in the vapor phase, to form silicon chlorides
3. reaction of silicon chlorides with carbon atoms to produce silicon carbide NW.

CCl_4 decomposition in the temperature range 767 – 1913 °C releases two chlorine atoms per decomposing molecule. In thermal plasmas in N_2 atmosphere the main species formed in the temperature range 477 – 1477 °C is chlorine (Huang & Guo, 2006). Either the main decomposition product is Cl_2 or Cl , a silicon extraction from the substrate is expected to occur due to the presence of halogens. This should be the result both of the surface etching (Dohnalek et al., 1994) and the reaction with the silicon vapor at the growth temperature.

All silicon chlorides, from $SiCl$ to $SiCl_4$, are expected to be formed in the gas phase, with different concentrations (Chaussende et al, 1999). These species react with the C formed by CCl_4 decomposition, giving silicon carbide. The growth of NW is catalyzed by the nickel atoms present on the silicon surface, according to the preferential interface nucleation mechanism (Wacaser et al., 2009).

This process produces NW several microns long, with diameters below 80 nm (see the secondary electron image in Fig. 10a). They are arranged into dense networks randomly oriented on the silicon surface. Some craters (Fig. 10b) are opened in the substrate surface due to the etching action of the chlorine, as mentioned above for the reaction process.

A first investigation of the SiC crystalline structure performed by X-ray diffraction (not shown here) confirms the presence of the characteristic peaks of the cubic SiC polytype, in particular the most intense (111) diffraction at $2\theta = 36.6^\circ$. In order to investigate the structure of the single NW, a more accurate structural characterization is carried out by TEM analyses. A typical low-magnification image of a single wire, with uniform diameter of about 50 nm, is shown in Fig. 11a. As verified by SAED and high resolution studies, the lattice is cubic (see Fig. 11b) and the NW growth axis is parallel to the [111] direction.

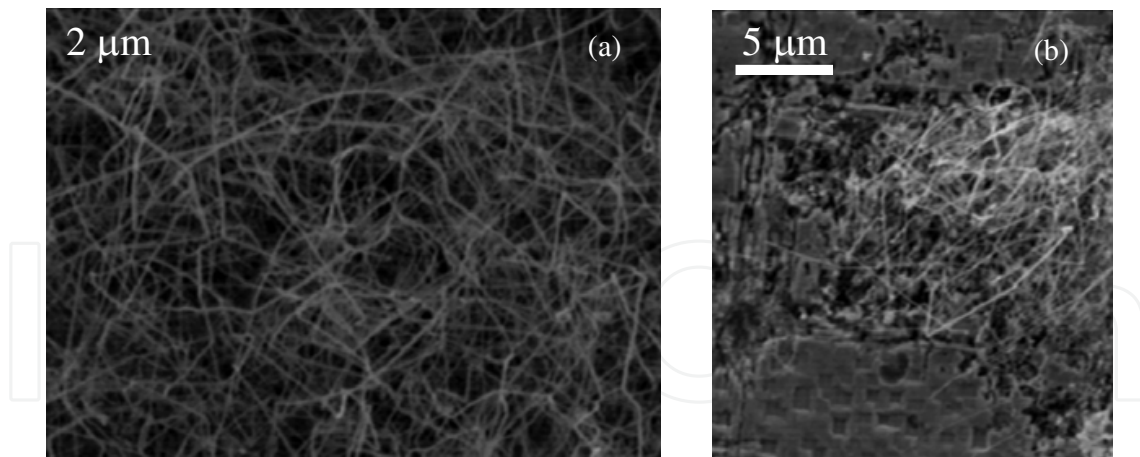


Fig. 10. SEM images showing (a) a typical NW ensemble, (b) the substrate surface etched by the chlorine.

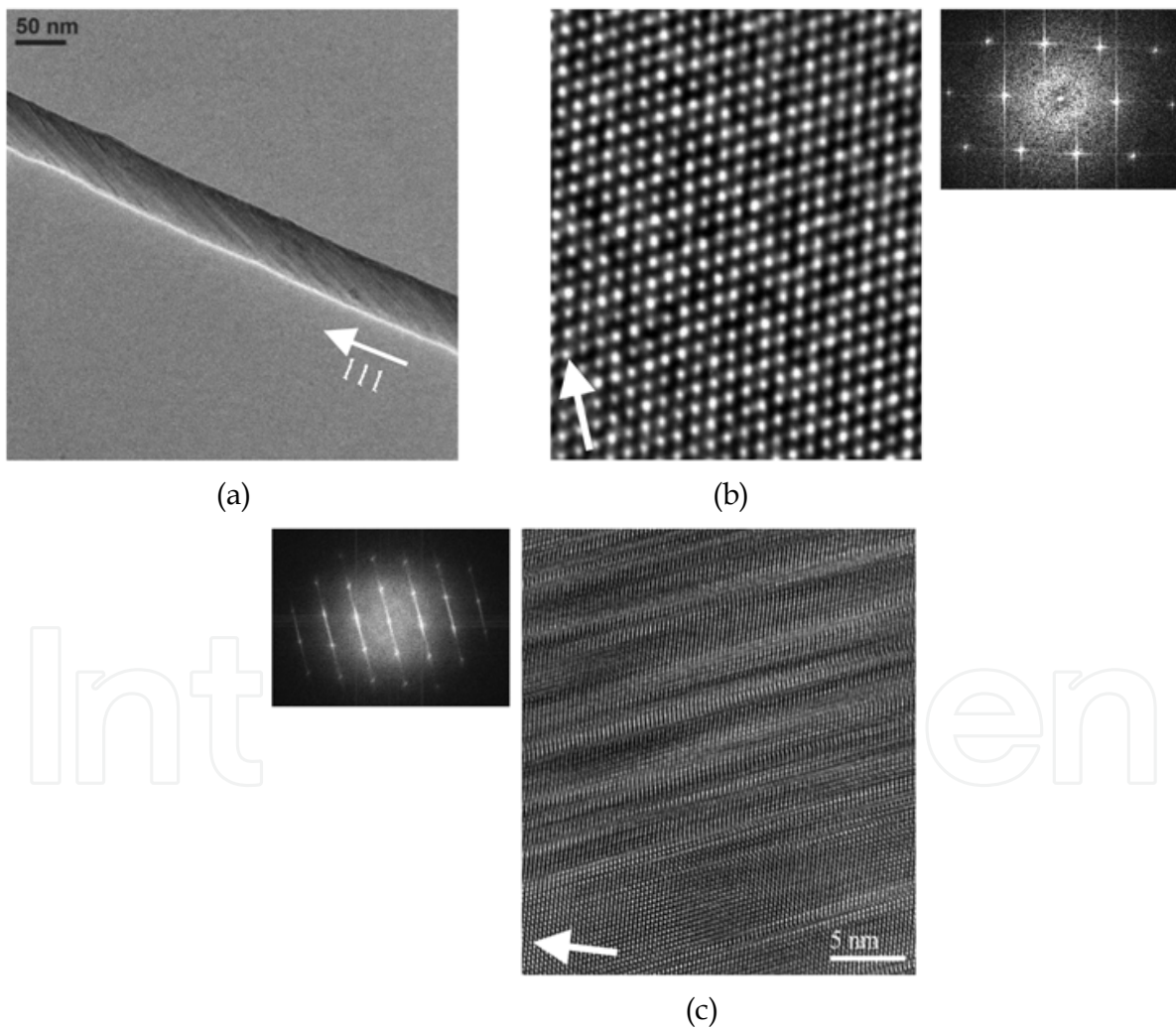


Fig. 11. (a) low magnification TEM image, (b) HRTEM image of a perfect region with its Fast Fourier Transform, (c) HRTEM image of a defective region with its Fast Fourier Transform. The crystal lattice is imaged in (b) and (c) along a $[110]$ zone axis. The arrows indicate the growth axis.

Defective areas are observed, a detail of which is shown in Fig. 11c, together with the corresponding streaky pattern in the power spectrum. These results are consistent with common findings on 3C-SiC whiskers, as discussed above for core/shell NW.

The CL emission spectrum of the NW ensemble (see Fig. 12) is quite broad. A Gaussian fitting and deconvolution was performed in order to resolve the different components. The peak related to the indirect band gap emission of the 3C-SiC NW is detected at 2.20 ± 0.02 eV. Two anomalous components, the band centered at 1.730 ± 0.005 eV and the dominant band at 1.950 ± 0.005 eV, are identified. A reference spectrum was acquired from a region of the substrate not covered by the NW, to eliminate possible contributions from porous silicon or silicon dioxide substrate. Since the luminescence from the substrate in this spectral region is about three orders of magnitude weaker, any spurious contribution can be excluded. In agreement with literature data, the emission at 1.73 eV can involve deep levels in 3C-SiC with activation energy of about 0.5 eV (Alfieri & Kimono, 2009; Itoh et al., 1997). The dominant red emission at about 1.95 eV can be tentatively assigned to the presence of substitutional oxygen on carbon site (O_C defects), unintentionally incorporated due to contaminants present in the open-tube growth (Gali et al., 2002). Finally, a high-energy emission is observed in the CL spectrum at 2.55 ± 0.02 eV. Luminescence above the band-gap in cubic SiC has been previously debated in the literature: attributions to quantum confinement effects in nanowhiskers (Zhang et al., 2002), effects of morphology, orientation, defects and dangling bonds in NW facets (Chen et al., 2008), or to recombination involving surface/interfacial groups (Shim et al., 1997) have been proposed. Since we have a typical NW size too large to achieve appreciable quantum confinement, the weak blue emission detected in CL could be more likely related to surface modifications.

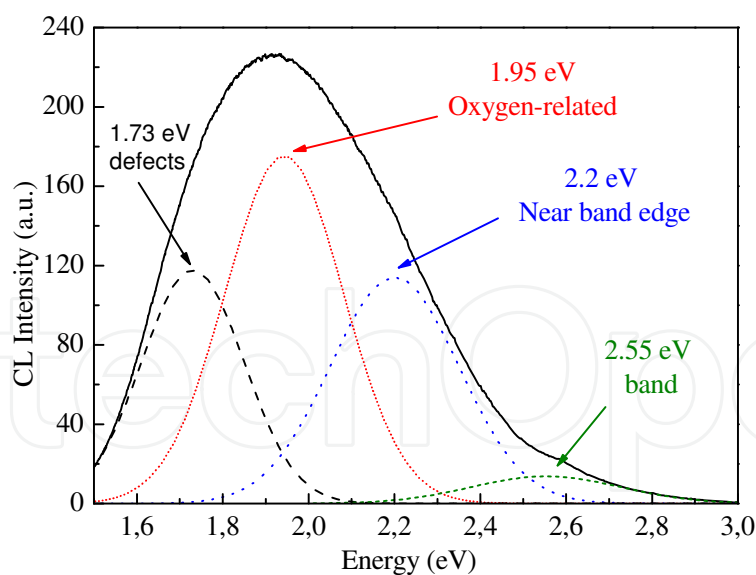


Fig. 12. CL spectrum at $T=77$ K of NW grown with CCl_4 precursor.

3.3 Growth of NW in VPE reactor

3C-SiC NW have been grown in a home-made induction heated Vapor Phase Epitaxy (VPE) reactor at atmospheric pressure (Fig. 13), by using diluted (3%) propane and silane as precursors, hydrogen as carrier gas and Ni as catalyst.



Fig. 13. Photo of the VPE reactor used to grow SiC NW.

A nominally 4 nm thick nickel film was deposited by e-beam evaporation system on a Si (100) substrate, previously etched in an HF solution for 60 s in order to remove the surface native oxide. For the VPE growth, a preheating of the nickel-deposited substrate at 1100°C for 2 minutes was performed in order to get catalyst dewetting, then the reagents were introduced into the growth chamber for a growth time of 5 minutes.

The process resulted in the formation of a NW network (Fig. 14a) in the nichel-covered substate areas. By spatially selective nichel deposition using conventional photolithographic techniques, peculiar geometries could be obtained (Fig. 14b).

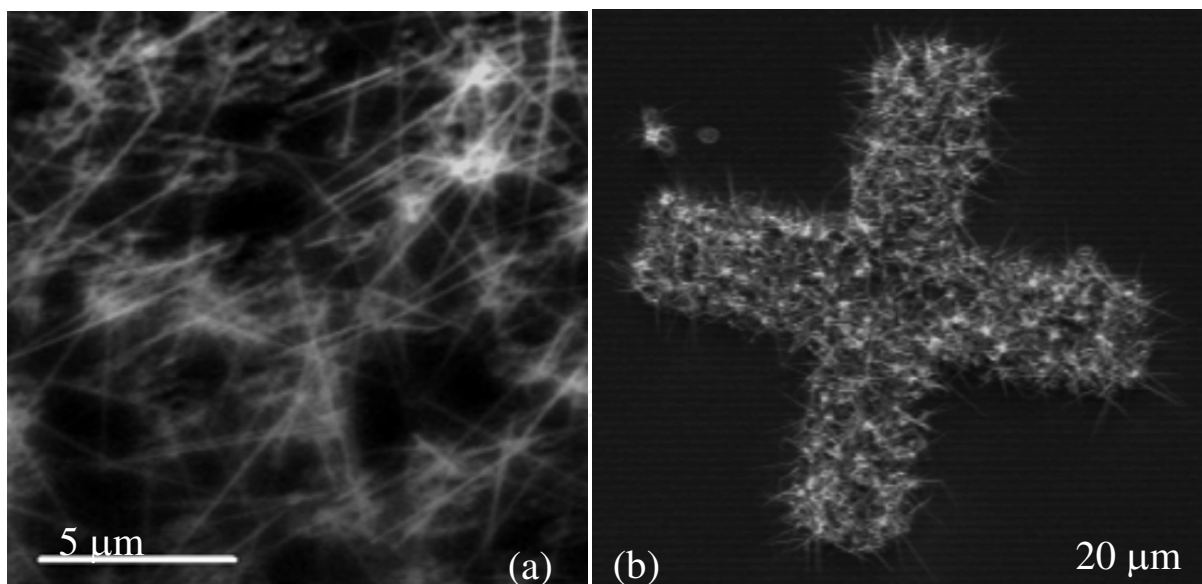


Fig. 14. SEM images of VPE grown NW. (a) NW network, b) selective NW growth in a cross-shaped area of the substrate.

Z-contrast analyses (Fig. 15) showed a high-Z (brightest) particle on top of the NW, indicating a metal-catalysed VLS growth mechanism. A tapering of the NW was observed: the average size decreases from about 80 nm in the center-base region to about 10 nm near the tip.

The lattice symmetry and structural quality of the as-grown NW were characterized by X-ray powder diffraction and TEM studies. The X-Ray profiles (not shown here) showed the characteristic peaks of β -SiC at $2\theta = 35.6^\circ$ (111), 41.4° (200), and 59.9° (220). The electron

diffraction patterns and the high-resolution TEM data confirmed the NW are predominantly 3C polytype with (111) growth axis, but stacking defects occur on (111) planes (Fig. 16a) and local stacking sequences characteristic of other polytypes (in particular 4H) are observed in the near-tip segments (Fig. 16b).

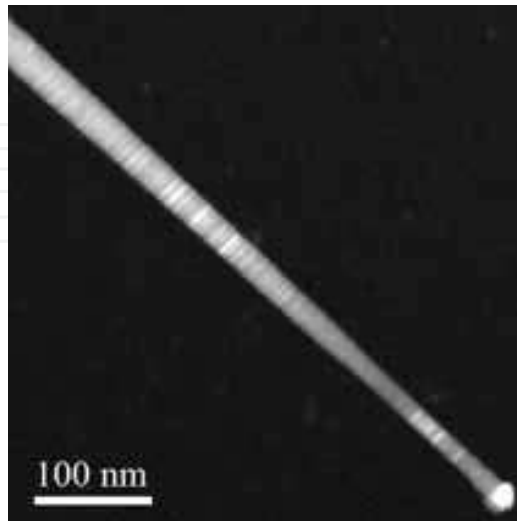


Fig. 15. TEM-HAADF (Z-contrast) image of a VPE grown NW.

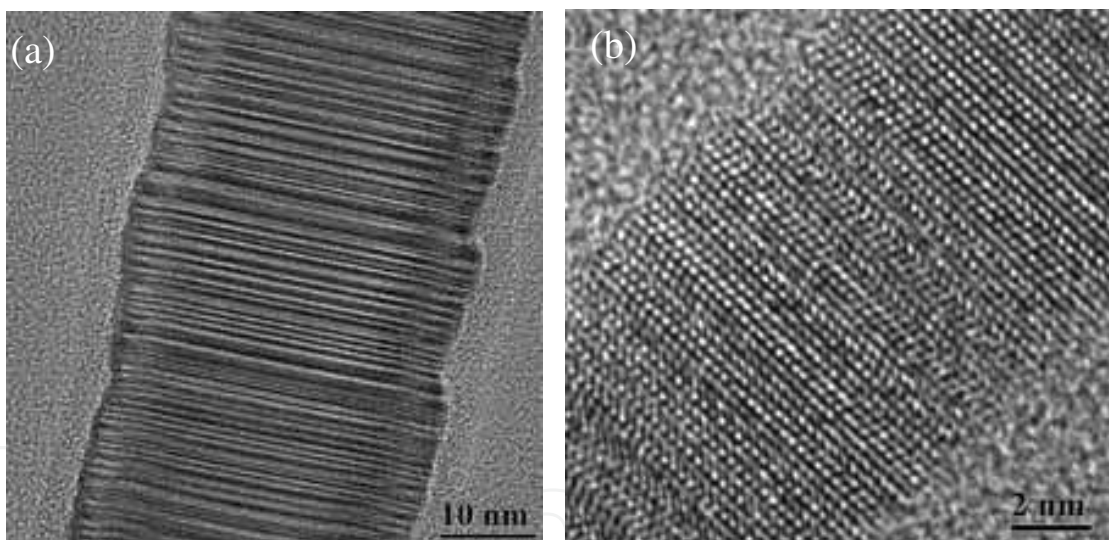


Fig. 16. HRTEM images in the center region (a) and in the tip region (b) of a VPE-grown NW.

The growth of NW was also tested on 3C-SiC substrates previously grown in the same reactor. The 3C-SiC film was deposited on 2" p-type (001) Si substrates. The substrate was etched in 10% HF solution for 60 s before introduction in the growth chamber and heated at 1000 °C for 10 minutes to completely remove the Si native oxide layer. In order to relax the lattice mismatch between SiC and Si, a carburisation step was performed before the growth: the temperature was lowered to 400 °C, 3 sccm of propane were injected in the growth chamber and the temperature was raised to 1100 °C in about 2 minutes. This temperature was then held for 5 minutes to complete the carburisation process and form a thin monocrystalline SiC layer on the Si substrate. After the carburisation process the propane flow is interrupted, the temperature is raised to 1200 °C and SiH₄ and C₃H₈ are injected in the growth chamber for 10 minutes (Bosi et al., 2009).

A Ni film, nominally 4 nm thick, was deposited on the 3C-SiC/Si wafer and the wires were grown in the same manner as described above.

A VLS nickel assisted growth of NW was achieved. A typical side-view SEM image is shown in Fig. 17a. The lattice structure and spacings (Fig. 17b) correspond to those of 3C-SiC, with stacking defects on (111) planes. At the tip, a quite sharp interface was observed between the SiC wire and the catalyst particle (magnified detail in Fig. 17c). TEM observation shows that zones with a lower defect density are observed on SiC NW grown on 3C-SiC with respect to the ones grown directly on Si.

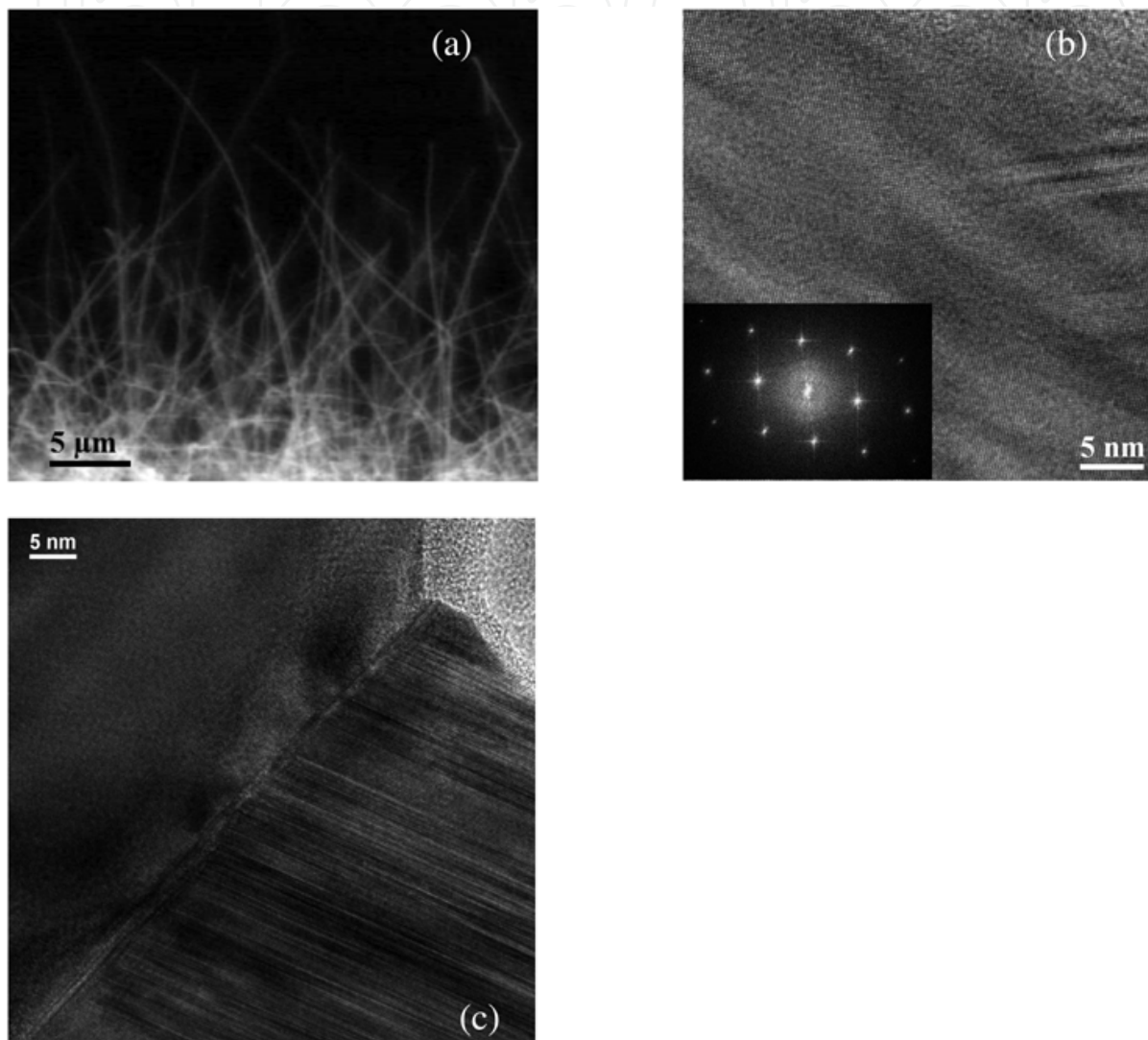


Fig. 17. (a) side-view SEM image of 3C-SiC NW grown on 3C-SiC substrate, (b) HRTEM image of the NW lattice and corresponding FFT analysis, (c) HRTEM image of the catalyst/wire interface at the tip.

4. Applications

The great interest that SiC has gathered in latest years is due the possibility to combine in one single material good semiconducting and chemical properties, biocompatibility and sensing potentiality. SiC chemical inertness, wide bandgap, tribological properties, hydroxyapatite-like osseointegration, and hemocompatibility make it a very promising

candidate for biosensors, interface with biological tissues and lab-on-chip medical devices. Moreover, the possibility to realize nanostructures opens the possibility to assemble novel nanoscale devices and arrays by the bottom-up approach, and to enhance the sensing capabilities of the material thanks to the high surface/volume ratio of NW.

As it happens with other materials, low dimensional SiC may exhibit peculiar electronic, optical, thermal and chemical properties, as well as carrier quantum confinement. Many mono-dimensional structures have proven to exhibit better properties than the same material with bulk size, and the bottom-up approach would permit to combine appropriate building blocks to obtain unique functions, or combinations of functions, in integrated nanosystems, unavailable in the conventional top-down approach.

Several electronic devices, such as power diodes or field-effect transistors based on 3C-SiC (SiCFET) have already been developed (Zhou et al. 2006a, Chung et al., 2008) and SiC power diodes have already reached the market stage (Roussel, 2007). Several devices are fabricated by thermally growing SiO₂ layer on n-type Si wafers followed by deposition of parallel Au contacts, used as source and drain electrodes, while the n-type silicon is used as back gate. n-type 3C-SiC FETs were tested at different temperatures and were proven to have good performance at high temperatures, with larger current and higher carrier mobility. SiC nanostructures could be used to enhance these landmarks even more, as it happened with other compounds, but very few literature papers deal with SiC NW applications, even if there are already several "proof of concept" nanodevices realized with conventional semiconductors such as Si, GaAs, GaN NW (Xia et al. 2006, Lieber & Wang, 2007).

One of the challenges for SiC research for the next years would involve using the experience gathered on other compounds in order to exploit SiC possibilities in nanoscience.

Large-scale β -SiC NW coated with SiO₂ layer exhibit the characteristics of an excellent photocatalyst. The photocatalytic activity was evaluated by the photocatalytic decomposition of gaseous acetaldehyde accompanied by generation of carbon dioxide. SiC/SiO₂ core/shell NW present higher photocatalytic activity than the pure 3C-SiC NW, resulting from their stronger absorption of gaseous acetaldehyde by SiO₂ and holes remaining in the valence band of SiC (Zhou et al., 2006b).

Functionalization of the SiC surface with specific organic or inorganic molecules is a possible route to obtain specific surface properties such as high selectivity, biomolecular recognition and adhesion of species of biological interest. SiC, in all its polytypes, is suggested as a suitable material for biofunctionalization of H-terminated surfaces via hydrosilylation similar to silicon (Yakimova et al., 2007). Experimental study of pyrrole functionalized Si- and C- terminated SiC have been made. This organic compound contains in its molecule NH group and two C-C double bond which may be used for further functionalizations (Preuss et al., 2006).

Other organic molecules with different functional groups, such as 3-aminopropyl triethoxysilane (APTES) having amine group or mercaptopropyl trimethoxysilane with thiol group, have been suggested for SiC NW surface functionalization.

In this framework we have used a Supersonic Molecular Beam Deposition approach (Milani & Iannotta, 1999) to functionalize 3C-SiC thick films and NW grown with our VPE reactor (Aversa et al., 2009). Porphyrins have been deposited onto the SiC surface and the core level/valence band emission have been studied with synchrotron radiation light. First experiments and analysis on SiC film show that both porphyrin macrocycle and the phenyl groups of the molecule have an interaction with the substrate: core level photoemission reveals significant changes on peak positions and lineshape. Functionalized 3C-SiC NW shows that oxidized and/or amorphous/oxy-carbide components are present, while the Si_{2p} and C_{1s} bands show a strong lineshape change. The interaction of attached molecules is

more evident on SiC NWs than on films, and a role of F in “etching” the outer shell of NW could be hypothesized.

MEMS are a family of technologies and integrated devices that are becoming more and more important in modern life. Some areas in which these systems are already applied are shock sensors for airbag, inkjet printers, accelerometers and gyroscopes for boats and airplanes, entertainment, healthcare instruments, communication and information technologies, biology and biosensors. MEMS offer significant advantages over hybrid systems and devices because of their small dimensions, integration of different components and low power consumption (Godignon & Placidi, 2007). Although Si is presently the most used material for MEMS fabrication it has serious limitations for some applications, such as high temperature ($T > 300\text{ }^{\circ}\text{C}$) and/or harsh environments with corrosive chemicals and biocompatibility, and SiC could be a viable alternative material. Micro cantilever of 3C-SiC with oscillating frequency in the order of 10^6 Hz and Q factors of 10^3 were realized and the resonators were used for high sensing applications such as mass detection for gas sensing devices in harsh environments (Zorman & Parro, 2008).

Combining MEMS and nanostructures peculiar characteristics such as high affinity to selected species via functionalization and high measurement sensitivity thanks to high resonant frequency and Q factors could open interesting possibility in detection devices for biological applications.

We have made some preliminary 3C-SiC NW depositions, starting from a patterned Si substrate on which structures such as micron-sized cantilever, beam and springs were fabricated. A Ni layer, nominally 2 nm thick, was deposited as catalyst on this microstructured Si substrate with an e-beam evaporator and the growth was performed in the VPE reactor, using the procedure described above. A SEM micrograph of the NW obtained on the spring is shown in fig. 18.

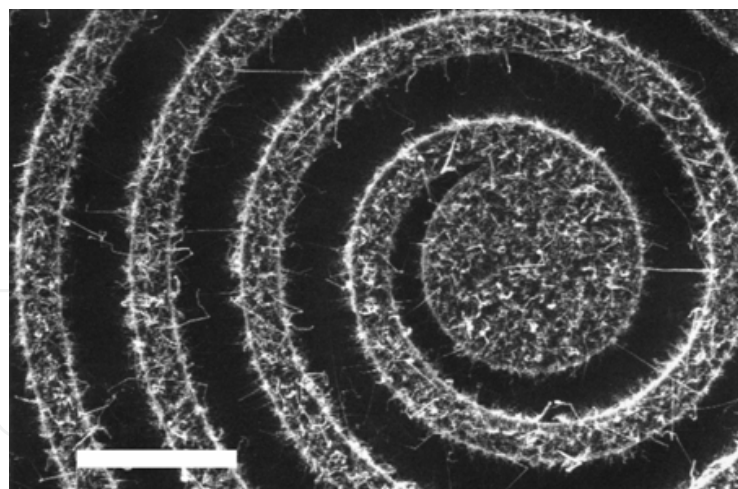


Fig. 18. SEM micrograph of 3C-SiC NW obtained on a Si spring (Si micromachined substrates were kindly provided by Dr. A. Roncaglia, IMM-Bologna, Italy). Marker is $20\text{ }\mu\text{m}$.

5. Conclusions

Nanowires (NWs) open promising near-future perspectives for the design and fabrication of nano-scale devices.

In this paper we discussed the 3C-SiC NW preparation obtained by three different growth procedures:

- SiC/SiO₂ core/shell NWs grown by a Chemical Vapor Deposition (CVD) process on n-type Si (001) substrates
- 3C-SiC (without shell) NWs obtained by a chemical reaction using carbon tetrachloride (CCl₄) as a precursor and Ni as catalyst.
- 3C-SiC NWs grown in an home-made Vapor Phase Epitaxy (VPE) reactor using propane and silane as precursors both diluted (3%) in hydrogen, and Ni as catalyst.

Selected morphological, structural and optical characterizations of the three NW sets, performed by Scanning Electron Microscopy, Transmission Electron Microscopy, X-Ray Diffraction and SEM-Cathodoluminescence, were presented.

We have presented some preliminary results about patterned NW growth on Si using standard photolithographic techniques to draw figures like crosses, NW functionalization using porphyrins and NW deposition on Si cantilever obtained by microstructuring a Si substrate.

6. Acknowledgements

We acknowledge the help of Mr. A. Motta for photolithographic work. Patterned SiC substrates were kindly provided by A. Roncaglia, IMM-CNR Bologna. We are grateful to Dr. L. Aversa, R. Verucchi and M. Nardi for synchrotron analysis.

7. References

- Afanas'ev V. V.; Bassler M.; Pensl G. & Schulz M. J. (1996). Band offsets and electronic structure of SiC/SiO₂ interfaces, *J Appl. Phys.*, Vol. 79, issue 6 (15 March 1996), pag. 3108-3114, ISSN: 0021-8979.
- Alfieri G. & Kimono T. (2009). Capacitance Spectroscopy Study of Midgap Levels in n-Type SiC Polytypes, *Mat. Sci. Forum*, Vol. 615 - 617 (March 2009) , pag. 389-392, ISSN: 0255-5476.
- Attolini, G., Rossi, F., Bosi, M., Watts, B. E. & Salviati, G. (2008). Synthesis and characterisation of 3C-SiC NW. *Jof non crystalline solid*, Vol. 354, issue 47-51 (1 December 2008) pag. 5227-5229, ISSN: 0022-3093
- Aversa L. , Verucchi R., Nardi M., Bosi M., Attolini G., Rossi F., Watts B., Nasi L., Salviati G., Iannotta S.: "SiC functionalization by porphyrin supersonic molecular beams", 26th European Conference on Surface Science (ECOSS), Parma, 30/8 - 4/9/2009.
- Bark, Y., Ryu, Y. & Yong K. (2006). Structural characterization of β -SiC nanowires synthesized by direct heating method. *Materials Science and Eng. C* Vol. 26, issue 5-7, Pag. 805-808, ISSN: 0928-4931
- Bechstedt F.; Kackell P.; Zywietz A.; Karch K.; Adolph B.; Tenelsen K. & Furthmuller (1997). Polytypism and properties of silicon carbide, *Phys. Stat. Sol. B*, Vol. 202 Issue 1 (16 November 1997), pag. 35-62, ISSN: 1521-3951.
- Bosi M.; Watts B. E.; Attolini G.; Ferrari C.; Frigeri C.; Salviati G.; Poggi A.; Mancarella F.; Roncaglia A.; Martnez O. & Hortelano V., 2009. Growth and Characterization of 3C-SiC Films for Micro Electro Mechanical Systems (MEMS) Applications, *Crystal Growth and Design*, DOI: 10.1021/cg900677c
- Casady J. B. & Johnson R. W. (1996) Status of silicon carbide (SiC) as a wide-bandgap semiconductor for high-temperature applications: a review, *Solid State Electronics*, Vol. 39, issue 10, pag. 1409-1422, ISSN: 0038-1101
- Chaussende, D.; Manteil, Y.; Aboughe-nze, P.; Brylinski, C. & Bouix, J (1999). Thermodynamical calculations on the chemical vapour transport of silicon carbide, *Mat Sci Eng B*, Vol. 30 (July 1999), pag. 98-101, ISSN: 0921-5107.

- Chen J.; Wu R.; Yang G.; Pan Y.; Lin J.; Wu L. & Zhai R. (2008). Synthesis and photoluminescence of needle-shaped 3C-SiC nanowires on the substrate of PAN carbon fiber. *J of Alloy and Compounds*, Vol. 456, issue 1-2, (25 February 2004), pag. 320-23, ISSN: 0925-8388.
- Choi, H-J.; Seong, H-K.; Lee, J-C. & Sung, Y-M (2004). Growth and modulation of silicon carbide NW. *Journal of crystal growth* Vol. 269, Issues 2-4 (1 September 2004), pag. 472-478, ISSN: 0022-0248.
- Chung G. S.; Ahn J. H. & Han K. B. (2008). Fabrication of poly 3C-SiC thin film diodes for extreme environment applications, *IEEE International Symposium on Industrial Electronics, 2008. ISIE 2008* (30 June 2008), pag. 2576-2579, ISBN: 978-1-4244-1665-3.
- Dohnalek, Z.; Gao, Q.; Choyke, W.J. & Yates Jr, J.T. (1994). Chemical reactions of chlorine on a vicinal Si (100) surface studied by ESDIAD, *Surf Sci*, Vol. 320, issue 3, 238-246, ISSN: 0039-6028.
- Gali A.; Heringer D.; Deak P.; Hajnal Z.; Frauenheim Th.; Devaty R.P. & Choyke W.J. (2002). Isolated oxygen defects in 3C- and 4H-SiC: A theoretical study, *Phys. Rev. B*, Vol. 66, Issue 12 (27 September 2002), pag. 125208-125215, ISSN: 1550-235x.
- Godignon P. & Placidi M. (2007). Recent improvements of SiC micro-resonators, *Phys. Stat. Sol. C*, Vol. 4, issue 4 (28 march 2007), Pag. 1548-1553, ISSN: 1610-1642.
- Huang, J.; Guo, W. & Xu, P. (2007). Comparative Study of Decomposition of CCl₄ in Different Atmosphere Thermal Plasmas, *Plasma Sci Technol*. Vol. 9, issue 1 (february 2007) pag. 76-79, ISSN: 1009- 0630.
- Itoh H.; Kawasuso A.; Ohshima T.; Yoshikawa M.; Nashiyama I.; Tanigawa S.; Misawa S.; Okumura H. & Yoshida S. (1997). Intrinsic Defects in Cubic Silicon Carbide, *Phys. Stat. Sol. (a)*, Vol. 162, Issue 1 (16 november 2001), pag. 173-198. ISSN: 1862-6319.
- Jabeen F.; Rubini S.; Grillo V.; Felisari L. & F. Martelli (2008). Room temperature luminescent InGaAs/GaAs core-shell nanowires, *Appl. Phys. Lett.*, Vol. 93, issue 8 (28 August 2008), pag. 083117 -083119, ISSN: 0003-6951.
- Kang, B.-C., Lee, S.-B. & Boo, J.-H. (2004). Growth of β -SiC NW on Si(100) substrates by MOCVD using nichel as a catalyst. *Thin Solid Films* Vol. 464-465, (October 2004), pag. 215-219, ISSN: 0040-6090
- Kassiba A.; Makowska-Janusik M.; Boucle J.; Bardeau J. F.; Bulou A. & Herlin-Boime N. (2002). Photoluminescence features on the Raman spectra of quasistoichiometric SiC nanoparticles: Experimental and numerical simulations, *Phys. Rev. B*, Vol. 66, issue 15 (14 October 2002), pag. 155317-155324, ISSN: 1550-235x.
- Khongwong, W., Imai, M., Yoshida K. & Yano, T. (2009). Influence of raw powder size, reaction temperature, and soaking time on synthesis of SiC/SiO₂ coaxial nanowires via thermal evaporation, *Journal of Ceramic Society of Japan*, Vol. 117, pag. 439-444, ISSN: 1348-6535
- Kolasinski, K.W. (2006). Catalytic growth of nanowires: Vapor-liquid-solid, vapor-solid-solid, solution-liquid-solid and solid-liquid-solid growth. *Curr. Opin. Solid State Mater. Sci.* vol. 10, issue 3-4, pag. 182-191, ISSN: 1359-0286.
- Li X. & Bhushan B. (1999). Micro/nanomechanical characterization of ceramic films for microdevices, *Thin Solid Films*, Vol. 340, issue 1, pag. 210-217, ISSN: 0040-6090.
- Liang, C.H., Meng, G.W., Zhand, L.D., Wu, Y.C. & Cui, Z. (2000). Large-scale synthesis of β -SiC nanowires by using mesoporous silica embedded with Fe nanoparticles, *Chem. Phys. Lett.* Vol. 329, issue 3-4 (20 October 2000) pag. 323-328. ISSN: 0009-2614
- Lieber C. M. & Wang Z. L. (2007). Functional Nanowires, *MRS Bull.*, Vol. 32 (february 2007), pag. 99-108, ISSN: 0883-7694.

- Louis C. ; Roux S.; Ledoux G. ; Dujardin C. ; Tillement O. ; Cheng B. L. & Perriat P. (2006). Luminescence enhancement by energy transfer in core-shell structures, *Chem. Phys. Lett.* Vol. 429, issue 1-3 (29 september 2006) pag. 157-160, ISSN: 0009-2614.
- M. Mehregany, C. A. Zorman, S. Roy, A. J. Fleischman, C. H. Wu, & N. Rajan (2000). Silicon Carbide for Microelectromechanical Systems, *Int. Mater. Rev.*, Vol. 45, issue 3, pag. 85-108, ISSN: 0950-6608
- Marshall, R.C., Faust J.W., & Ryan, C.E.; (1973) Silicon carbide; *Proceedings of the International Conference on Silicon Carbide* Columbia : University of South Carolina Press, ISBN 0872493156.
- McKnight S.W. & Palik E.D. (1980). Cathodoluminescence of Films, *J Non-Crystal. Solids*, Vol. 40, issue 1-3, pag. 595-604, ISSN: 0022-3093.
- Meng, A., Li, Z., Zhang, J., GaO, L. & Li, H. (2007). Synthesis and Raman scattering of β -SiC/SiO₂ core-shell nanowires, *J Cryst. Growth*. Vol. 308, issue 2, (15 October 2007) pag. 263-268, ISSN: 0022-0248
- Milani P. & Iannotta S. (1999). *Cluster Beam Synthesis of Nanostructured Materials (Series in Cluster Physics, 1)* Springer, ISBN: 3540643702.
- Nakashima S. & Harima H. (1997). Raman investigation of SiC polytypes, *Phys. Stat. Sol. A*, Vol. 162, Issue 1 (16 November 1997), pag. 39-64, ISSN: 1862-6319
- Pistol M.E. & Pryor C.E. (2008). Band structure of core-shell semiconductor nanowires, *Phys. Rev. B*, Vol. 78, issue 11 (23 September 2008), pag. 115319, ISSN: 1550-235x.
- Preuss, M.; Bechstedt, F.; Schmidt, W.G.; Sochos, J.; Schroter, B. & Richter, W. (2006). Clean and pyrrole-functionalized Si- and C-terminated SiC surfaces: First-principles calculations of geometry and energetics compared with LEED and XPS, *Phys. Rev. B*, Vol. 74, issue 23 (December 2006), pag. 235406 ISSN: 1550-235x.
- Roussel, P, Semiconductor Today vol. 2, issue 5, 2007, pag.40 - <http://www.semiconductor-today.com/features/Semiconductor%20Today%20-%20SiC%20power%20devices.pdf>
- Sarro P. M. (2000). Silicon carbon as a new MEMS technology, *Sens. Actuators A*, vol. 82, issue 1-3, pag. 210-218, ISSN: 0924-4247
- Seo, W. -S.; Koumoto, K. & Aria, S. (2000). Morphology and Stacking Faults of-SiC Whisker Synthesized by Carbothermal Reduction, *J Am. Ceram. Soc.* Vol. 83, issue 10, pag. 2584-2592, ISSN 0002-7820.
- Seong, H-K,; Choi, H-J.; Lee, S-K.; Lee, J-I. & Choi, D-J. (2004). Optical and electrical transport properties in silicon carbide NW. Applied Physics Letters, vol. 85, issue 7 (August 2004), pag. 1256-1258, ISSN: 0003-6951.
- Shim H.W.; Kim K.C.; Seo Y.H.; Nahm K.S.; Suh E.K.; Lee H.J. & Hwang Y.G. (1997) Anomalous photoluminescence from 3C-SiC grown on Si(111) by rapid thermal chemical vapor deposition. *Appl. Phys. Lett.* Vol. 70, issue 13 (31 march 1997), pag. 1757-59. ISSN: 0003-6951.
- Skold N.; Karlsson L.S.; Larsson M.W.; Pistol M.E.; Seifert W.; Tragardh J. & L. Samuelson (2005). Growth and Optical Properties of Strained GaAs-Ga_xIn_{1-x}P Core-Shell Nanowires, *Nanolett.*, Vol. 5, issue 10 (13 September 2005), pag. 1943-1947, ISSN: 1530-6984.
- Skuja L. (1998). Optically active oxygen-deficiency-related centers in amorphous silicon dioxide, *J Non-Crystal. Solids*, Vol. 239, pag. 16-48, ISSN: 0022-3093.
- Takai, S., Kohno, H. & Takeda, S. (2007). MOCVD growth of SiC NW aiming at the control of their shape. *Advanced Materials Research*, Vol. 26-28, Pag. 657-660, ISSN: 1022-6680
- Tomioka K.; Kobayashi Y.; Motohisa J.; Hara S. & T. Fukui (2009). Selective-area growth of vertically aligned GaAs and GaAs/AlGaAs core-shell nanowires on Si(111) substrate, *Nanotechnol.* Vol. 20 Issue 14 (April 2009), pag. 145302-145305, ISSN:0957-4484.

- Wacaser, B.A.; Dick, K.A.; Johansson, J.; Borgstrom, M.T.; Deppert, K. & Samuelson L. (2009). Preferential Interface Nucleation: An Expansion of the VLS Growth Mechanism for Nanowires, *Adv. Mater.* Vol. 21, Issue 2 (25 November 2008), pag. 153-165, ISSN: 1521-4095.
- Wagner, R. S. & Ellis W.C. (1964). Vapor-liquid-solid mechanism of single crystal growth, *Appl. Phys. Lett.* Vol. 4, pag. 89, ISSN: 0003-6951
- Wang N., Cai Y., & Zhang R.Q. (2008). Growth of nanowires, *Mater. Sci. Eng. R.* Vol. 60, issue 1-6, pag. 1-51, ISSN: 0927-796X
- Willander M., Friesel M., Whahab Q-U & Straumal B. (2006), Silicon carbide and diamond for high temperature device applications, *J Mater. Sci: Mater. El.*, Vol. 17, issue 1, pag. 1-25, ISSN: 0957-4522
- Xi G., Liu Y., Liu X., Wang X. & Qian Y. (2006). Mg-catalyzed autoclave synthesis of aligned silicon carbide nanostructures. *Phys. Chem. B*, Vol. 110, issue 29 (Jul 2006), pag. 14172-14178, ISSN: 1089-5647.
- Xia B. Y.; Yang P.; Sun Y.; Wu Y.; Mayers B.; Gates B.; Yin Y.; Kim F. & Yan H. (2003). One-dimensional nanostructures: synthesis, characterization and applications, *Adv. Mater.* Vol. 15. issue 5 (march 2004), pag. 353-389, ISSN: 1521-4095.
- Yakimova R., Petoral R. M., Yazdi G. R., Vahlberg C., Petz A. L. & Uvdal K. (2007). Surface functionalization and biomedical applications based on SiC, Surface functionalization and biomedical applications based on SiC, *J Phys. D: Appl. Phys.* Vol. 40, pag. 6435-6442. ISSN: 0022-3727
- Yang, L.; Zhang, X.; Huang, R.; Zhang, G. & Xue, C. (2006). Formation of β -SiC NW by annealing SiC films in hydrogen atmosphere. *Physica E*, Vol. 35, Issue: 1 (October 2006), pag. 146-150, ISSN: 1386-9477.
- Yang, W.; Araki, H.; Kohyama, A.; Thaveethavon S.; Suzuki, H. & Noda, T. (2004). Fabrication in-situ NW/SiC matrix composite by chemical vapour infiltration process. *Materials Letters*, Vol. 58, Issue 25 (October, 2004), Pag. 3145-3148, ISSN 0167-577X.
- Yoshida H.; Kohno H; Ichikawa S.; Akita T. & S. Takeda (2007). Inner potential fluctuation in SiC nanowires with modulated interior structure, *Mat. Lett.* Vol. 61, Issue 14-15 (June 2007), pag. 3134-3137, ISSN: 0167-577X
- Zhang Y.; Nishitani-Gamo M.; Xiao C. & Ando T. (2002) Synthesis of 3C-SiC nanowhiskers and emission of visible photoluminescence. *J. Appl. Phys.* Vol. 91, issue 9 (1 may 2002), pag. 6066-6070. ISSN: 0021-8979.
- Zhang, H-F., Wang, C-M. & Wang, L-S. (2002). Helical Crystalline SiC/SiO₂ Core- Shell Nanowires, *Nano Letters* Vol. 2, issue 9, (26 July 2002), pag. 941-944. ISSN: 1530-6984
- Zhou, W.M.; Fang, F.; Hou, Z.Y.; Yan, L.J. & Zhang, Y.F. (2006a). *Fiel-Effect transistor based on β -SiC NW.* *IEEE Electron Device Letters*, Vol. 27, issue 6 (june 2006), pag. 463-465. ISSN: 0741-3106.
- Zhou, W.; Yan, L.; Wang, Y. & Zhang, Y.; (2006b) Sic NW: a photocatalytic nanomaterial. *Appl. Phys. Lett.*, Vol. 89, issue 1 (5 july 2006), pag. 013105, ISSN: 0003-6951.
- Zhu J.; Liu S. & Liang J. (2000). Raman study on residual strains in thin 3C-SiC epitaxial layers grown on Si(001), *Thin Solid Films*, Vol. 368, Issue 2 (15 June 2000, pag. 307-311, ISSN: 0040-6090.
- Zhu, S.; Xi, H-A.; Li, Q. & Wang, R.; (2005) In situ growth of β -SiC NW in porous SiC ceramics. *Journal Am. Ceram. Soc.* Vol 88, Issue 9 (September 2005), pag. 2619-2621, ISSN 0002-7820
- Zorman C.; & Parro R. (2008). Micro- and nanomechanical structures for silicon carbide MEMS and NEMS, *Phys. Stat. Sol (b)*, Vol. 245, issue 7 (July 2008), pag. 1404-1424, ISSN: 1521-3951.



Nanowires

Edited by Paola Prete

ISBN 978-953-7619-79-4

Hard cover, 414 pages

Publisher InTech

Published online 01, February, 2010

Published in print edition February, 2010

This volume is intended to orient the reader in the fast developing field of semiconductor nanowires, by providing a series of self-contained monographs focusing on various nanowire-related topics. Each monograph serves as a short review of previous results in the literature and description of methods used in the field, as well as a summary of the authors recent achievements on the subject. Each report provides a brief sketch of the historical background behind, the physical and/or chemical principles underlying a specific nanowire fabrication/characterization technique, or the experimental/theoretical methods used to study a given nanowire property or device. Despite the diverse topics covered, the volume does appear as a unit. The writing is generally clear and precise, and the numerous illustrations provide an easier understanding of the phenomena described. The volume contains 20 Chapters covering altogether many (although not all) semiconductors of technological interest, starting with the IV-IV group compounds (SiC and SiGe), carrying on with the binary and ternary compounds of the III-V (GaAs, AlGaAs, GaSb, InAs, GaP, InP, and GaN) and II-VI (HgTe, HgCdTe) families, the metal oxides (CuO, ZnO, ZnCoO, tungsten oxide, and PbTiO₃), and finishing with Bi (a semimetal).

How to reference

In order to correctly reference this scholarly work, feel free to copy and paste the following:

Giovanni Attolini, Francesca Rossi, Filippo Fabbri, Matteo Bosi, Giancarlo Salviati and Bernard Enrico Watts (2010). Cubic SiC Nanowires: Growth, Characterization and Applications, Nanowires, Paola Prete (Ed.), ISBN: 978-953-7619-79-4, InTech, Available from: <http://www.intechopen.com/books/nanowires/cubic-sic-nanowires-growth-characterization-and-applications>

INTECH
open science | open minds

InTech Europe

University Campus STeP Ri
Slavka Krautzeka 83/A
51000 Rijeka, Croatia
Phone: +385 (51) 770 447
Fax: +385 (51) 686 166
www.intechopen.com

InTech China

Unit 405, Office Block, Hotel Equatorial Shanghai
No.65, Yan An Road (West), Shanghai, 200040, China
中国上海市延安西路65号上海国际贵都大饭店办公楼405单元
Phone: +86-21-62489820
Fax: +86-21-62489821

© 2010 The Author(s). Licensee IntechOpen. This chapter is distributed under the terms of the [Creative Commons Attribution-NonCommercial-ShareAlike-3.0 License](https://creativecommons.org/licenses/by-nc-sa/3.0/), which permits use, distribution and reproduction for non-commercial purposes, provided the original is properly cited and derivative works building on this content are distributed under the same license.

IntechOpen

IntechOpen